Chapter 10
Active Damping

10.1 Introduction

As indicated in the introduction of the book, Sect. 1.3, passive dampers despite that they provide a good attenuation over a wide band of frequencies, they always have a significant resonance peak at a certain frequency within the frequency range of operation. To correct this situation an active vibration isolation (control) has to be considered. The test bench described in Sect. 2.1, belongs to this category. Such a system has a primary path through which the disturbances are attenuated in certain frequency ranges and amplified around the resonance of the system. The secondary path is expected to correct the behaviour of the primary path in the frequency region where the primary path shows a significant resonance (amplification of the vibrations in this zone) through the appropriate use of feedback control. The use of the feedback should attenuate the effect of the resonance of the primary path without deteriorating the attenuation provided by the primary path at other frequencies. This means that the "water bed" effect due to the Bode integral should be carefully managed by shaping the sensitivity functions. Recall also that active damping consists of damping a resonance mode without changing its frequency.

The methodology of designing active damping systems will be illustrated by considering the active suspension described in Sect. 2.1.

The first step of the design consists of defining the control specifications. Roughly, the control objective is illustrated in Fig. 10.1 where the PSD (power spectral density) of the residual force is represented (thin line). We would like to attenuate the resonance but it is the meantime that the tolerated amplification at other frequencies with respect to the open-loop characteristics should be very low.[1] The desired template for the PSD corresponds to the curve in thick grey line is shown in Fig. 10.1. The final objective of the design will be to find the lowest complexity controller which allows matching the performance specifications.

[1] As a consequence of the Bode integral, the level of attenuation imposed is related to the level of tolerated amplification at other frequencies.

I.D. Landau et al., *Adaptive and Robust Active Vibration Control*,
Advances in Industrial Control, DOI 10.1007/978-3-319-41450-8_10

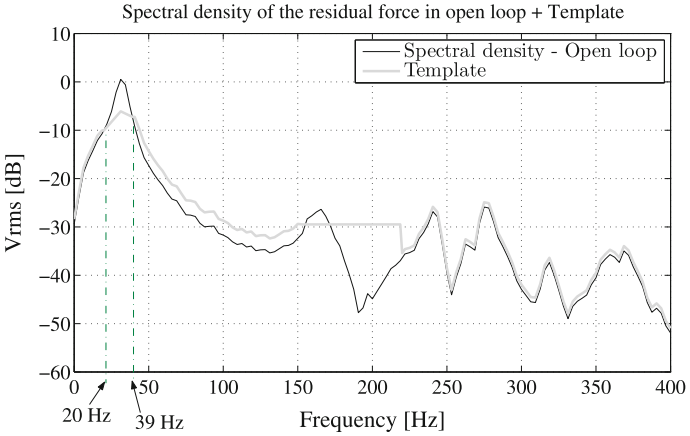

Fig. 10.1 Template imposed on the spectral density of the residual force

Once the performance specifications are formulated, the methodology of design is illustrated in Fig. 10.2. It comprises a number of steps:

- Open-loop identification of the secondary path (one needs a model of the secondary path for controller design).
- Design of a robust controller allowing to match the performance specifications (the design uses the model identified in open-loop operation).
- Implementation and test.
- Identification of the secondary path model in closed-loop operation (an improved model is expected).
- Redesign (retuning) of the controller based on the model identified in closed-loop operation.
- Implementation and validation of the new controller.
- Controller order reduction preserving the stability and performance of the system.
- Implementation and validation of the reduced order controller.

It may happen in practice that one stops after the test of the controller designed on the basis of the model of the secondary path identified in open-loop operation; however, once the implementation of the controller is done it is easy to do an identification in closed loop and the procedure can go further. The complexity controller reduction may not be necessary in some cases if there are no constraints on the computer power or on the cost of the control.

10.2 Performance Specifications

In active damping the desired performances are specified in the frequency domain. A template for the expected power spectral density (PSD) of the residual force or acceleration has to be defined. For the active suspension described in Sect. 2.1, the desired template is shown in Fig. 10.1 and the details are given below:

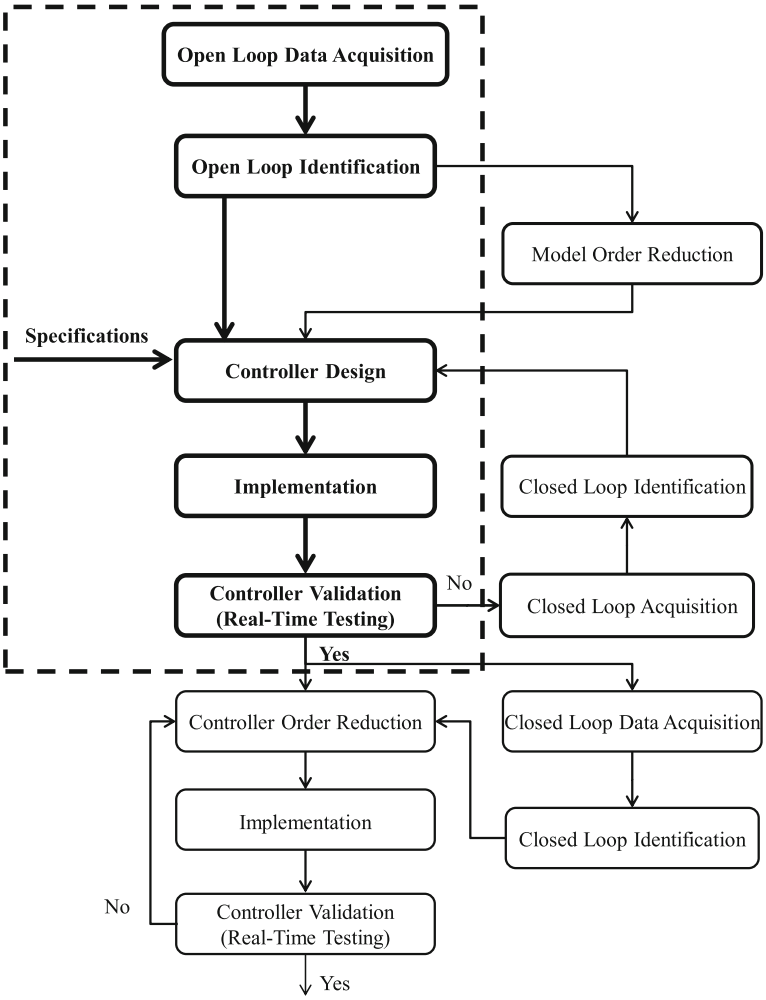

Fig. 10.2 Design methodology

- for frequencies below 20 Hz, maximum amplification with respect to the open loop: 1 dB;
- at 20 Hz, 0 dB amplification;
- at 31.25 Hz (the resonance) an attenuation of at least 6.6 dB;
- at 39 Hz, maximum 0 dB amplification;
- between 39 and 150 Hz maximum 3 dB amplification with respect to the open-loop PSD;
- between 150 and 220 Hz amplification/attenuation below −30 dB with respect to the value of the open-loop PSD at the resonance; and

- from 220 Hz above, maximum amplification of 1 dB with respect to the open-loop PSD.

In addition, as for any feedback control systems, robust specifications should be considered:

- modulus margin ≥ -6 dB;
- delay margin ≥ 1.25 ms (one sampling period);
- $S_{up} < 10$ dB, between 0 and 35 Hz; $S_{up} < 0$ dB, between 40 and 150 Hz; $S_{up} < -20$ dB, between 150 and 220 Hz and < -30 dB above 220 Hz; and
- opening the loop at 0.5 f_s.

The reduction of the magnitude of S_{up} is related to the robustness with respect to additive uncertainties and the fact that the system has low gain in high frequencies (robustness requires low level control action at the frequencies where the system has no gain—see Sect. 7.2). Opening the loop at 0.5 f_s will lower drastically the gain of the controller at high frequencies close to 0.5 f_s.

One of the steps in the design procedure is to transform the objectives shown in Fig. 10.1 and detailed above in specifications for the design of the feedback system. The active damping can be interpreted as an additional attenuation/amplification of the disturbance (vibration) acting upon the system. In other terms the difference between the PSD of the residual force in open-loop operation and the desired PSD will give the desired attenuation and the tolerated amplification for the feedback loop around the secondary path. The attenuation/amplification introduced by a feedback system is characterized by the frequency domain behaviour of the output sensitivity function S_{yp}. Therefore the difference between the open-loop PSD of the residual acceleration (force) and the desired PSD will generate a *desired template* for the modulus of the output sensitivity function to be achieved. Figure 10.3 shows the

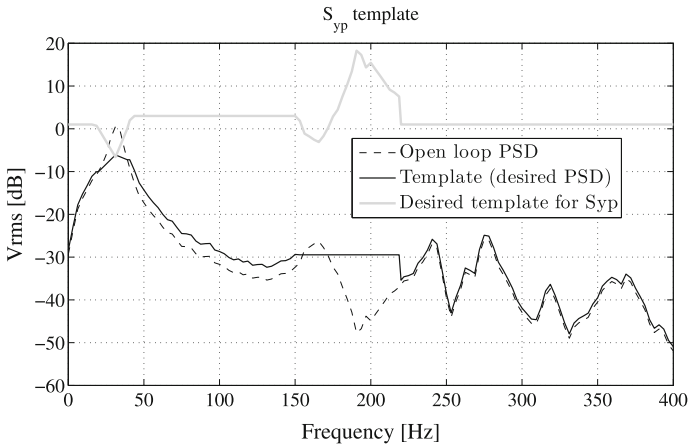

Fig. 10.3 Desired template for the output sensitivity function S_{yp} (without the robustness constraints)

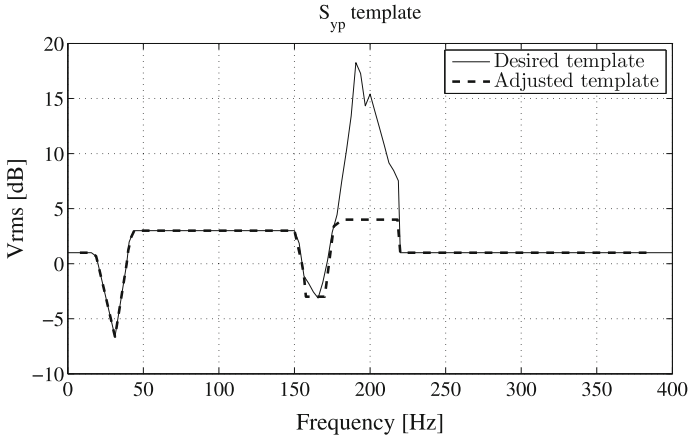

Fig. 10.4 Desired template for the output sensitivity function S_{yp} and adjusted template taking into account the robustness constraints

open-loop PSD, the desired PSD when active damping operates and their difference which constitutes a first template for the desired output sensitivity function.

Nevertheless, this template has to take into account also the robustness constraints imposed in terms of modulus margin and delay margin. Modulus margin imposes a maximum of 6 dB and this maximum decreases in high frequencies as a consequence of the constraints on the delay margin. Figure 10.4 shows the desired template as well as the adjusted one which takes into account the modulus and the delay margins. Figure 10.5 shows the template for shaping the input sensitivity function resulting from the specifications defined earlier (nominal template).

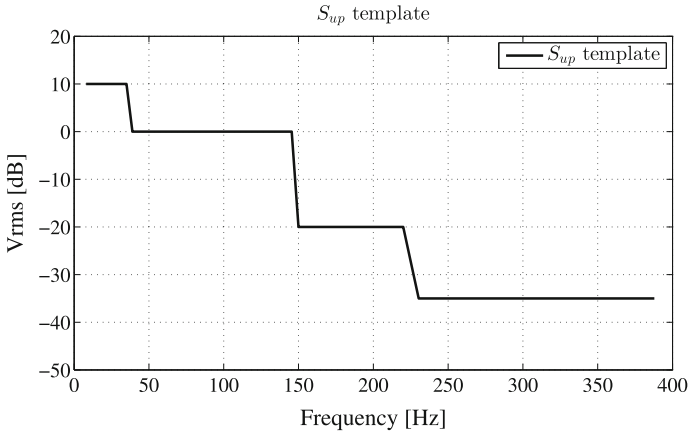

Fig. 10.5 Template for the input sensitivity function S_{up}

10.3 Controller Design by Shaping the Sensitivity Functions Using Convex Optimization

The convex optimization procedure for controller design has been presented in Sect. 7.4. Since the objective is also to obtain a low complexity controller, a first step which was considered in this approach was to use a reduced order secondary path model taking into account that according to the control objective, the control will not have to be effective in high frequencies. One of the most commonly used and efficient methods for model reduction is balancing. Because in the case of the active suspension we are interested in specific frequency intervals, the approach considered for the model reduction is the frequency-weighted balancing method which is suitable when a certain frequency range is of interest. Given the nominal full order model G and the input and output weighting matrices W_i and W_o, the objective is to find a stable and minimum-phase lower order model G_r such that the weighted error

$$\|W_o(G - G_r)W_i\|_\infty \tag{10.1}$$

is as small as possible.

The identified model of the secondary path has been presented in Sect. 6.1.1. A reduced order model with $n_A = 8$, $n_B = 11$, $d = 0$ has been obtained by using the "balanced truncation" technique in which the low frequencies have been appropriately weighted. The parameters of the reduced order model are given in Table 10.1. The frequency characteristics of the nominal and reduced order models are shown in Fig. 10.6.

Nevertheless, once the design is done on the reduced order model, the resulting controller has to be tested on the full order model before implementation. After a

Table 10.1 Parameters of the reduced order model

Coeff.	A	Coeff.	B
a_0	1.0000	b_0	0.0000
a_1	−2.1350	b_1	0.1650
a_2	2.1584	b_2	−1.0776
a_3	−2.2888	b_3	3.6137
a_4	2.2041	b_4	−8.1978
a_5	−1.8433	b_5	15.4346
a_6	1.4035	b_6	−19.4427
a_7	−0.2795	b_7	14.2604
a_8	−0.2057	b_8	−10.8390
a_9	–	b_9	11.9027
a_{10}	–	b_{10}	−7.2010
a_{11}	–	b_{11}	1.3816

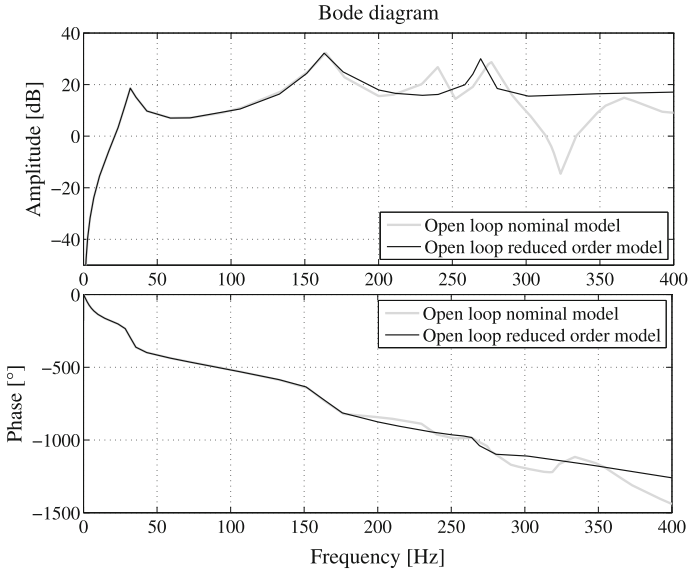

Fig. 10.6 Bode diagram (amplitude and phase) of the open-loop nominal and reduced order models

trial it was found that the basic templates have to be modified in certain frequency regions in order that the controller designed on the reduced order model matches the original templates when used with the nominal full order model.

For initializing the optimization procedure for controller design, a pair of poles at the resonance frequency $f = 31.939$ Hz with a damping $\xi = 0.8$, and a fixed real pole corresponding to the lowest frequency pole of the system (located at the intersection of the 5.73 Hz curve with the real axis) have been assigned. The region of optimization for the poles has been considered to be a circle with a radius 0.99. A fixed part in the controller $H_R = 1 + q^{-1}$ is introduced in order to open the loop at 0.5 f_s.

For convenience, the controller designed will be denoted OLBC (**O**pen **L**oop **B**ased **C**ontroller—controller designed using the open-loop identified model). The parameters of the resulting OLBC controller ($n_R = 27$, $n_S = 30$) are given in Table 10.2.

In Fig. 10.7, the achieved sensitivity functions with the full nominal model are shown. Clearly, the controller allows matching the specifications. The achieved modulus margin is -2.775 dB and the achieved delay margin is 4.1 T_s ($T_s = 1.25$ ms).

The performance on the real system is shown in Fig. 10.8. As it can be seen the specifications are satisfied.

Nevertheless, the full design procedure will be illustrated since in certain cases:

- the results obtained with the controller designed on the basis of the open-loop model may not necessarily be fully satisfactory; and
- the complexity of the controller has to be reduced.

Table 10.2 Parameters of the controller based on the reduced order open-loop identified model (OLBC)

Coeff.	R	Coeff.	S	Coeff.	R	Coeff.	S
r_0	0.0162	s_0	1.0000	r_{16}	0.0071	s_{16}	−0.1070
r_1	−0.0515	s_1	−5.1406	r_{17}	−0.0111	s_{17}	0.1031
r_2	0.0695	s_2	11.9134	r_{18}	−0.0068	s_{18}	−0.0384
r_3	−0.0255	s_3	−15.9616	r_{19}	0.0263	s_{19}	0.1284
r_4	−0.0666	s_4	12.7194	r_{20}	−0.0198	s_{20}	−0.0601
r_5	0.1315	s_5	−4.5490	r_{21}	0.0032	s_{21}	−0.0939
r_6	−0.1245	s_6	−2.0666	r_{22}	−0.0059	s_{22}	0.0027
r_7	0.0570	s_7	3.1609	r_{23}	0.0188	s_{23}	0.1820
r_8	0.0485	s_8	0.7437	r_{24}	−0.0180	s_{24}	−0.1586
r_9	−0.1405	s_9	−6.0665	r_{25}	0.0066	s_{25}	0.0457
r_{10}	0.1456	s_{10}	8.5544	r_{26}	0.0003	s_{26}	−0.0534
r_{11}	−0.0610	s_{11}	−6.8795	r_{27}	−0.0007	s_{27}	0.1081
r_{12}	−0.0242	s_{12}	3.6997	r_{28}	–	s_{28}	−0.0901
r_{13}	0.0422	s_{13}	−1.8094	r_{29}	–	s_{29}	0.0345
r_{14}	−0.0212	s_{14}	1.0885	r_{30}	–	s_{30}	−0.0049
r_{15}	0.0051	s_{15}	−0.4045	–	–	–	–

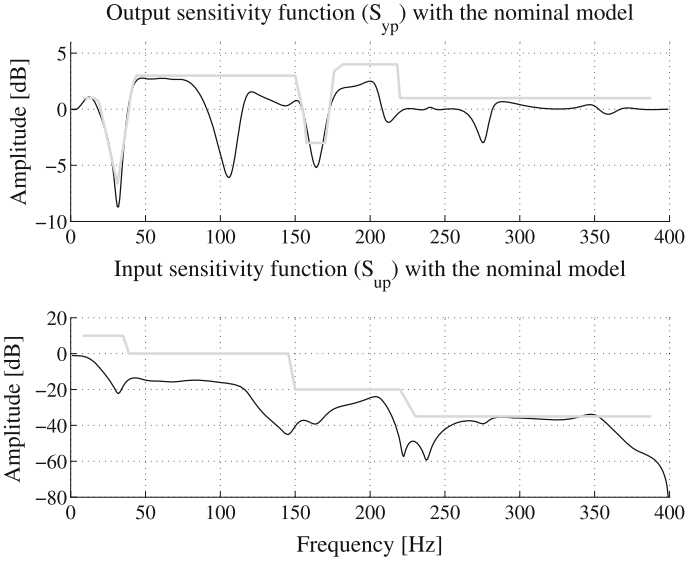

Fig. 10.7 Achieved sensitivity functions (*black*) with the OLBC controller and the nominal model

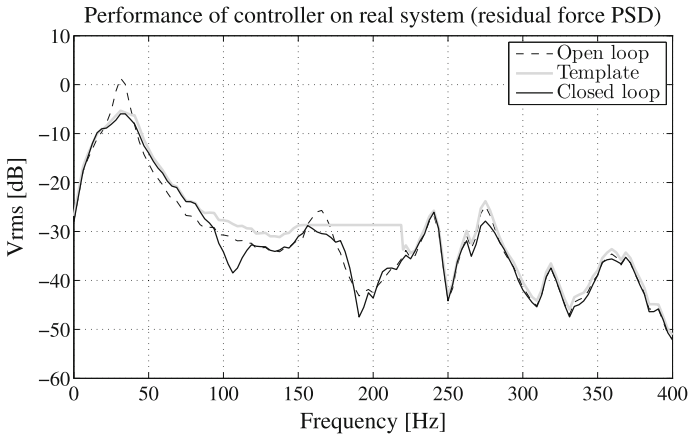

Fig. 10.8 Performance of the OLBC controller on the real system (PSD of the residual force)

10.4 Identification in Closed-Loop of the Active Suspension Using the Controller Designed on the Model Identified in Open-Loop

The methodology of identification in closed-loop operation has been presented in Chap. 8. A model with $n_A = 14$, $n_B = 16$ and $d = 0$ will be identified (same orders as for the model identified in open-loop operation).

One would like to identify a model which will minimize the error between the true output sensitivity function and the estimated sensitivity function, taking also into account that the plant model has a double differentiator. To achieve this, the excitation has been added to the input of the filter R (see Chap. 8 for details). Within this context, data acquisition was done with the same PRBS sequence as in open-loop identification (generated by 9-bit shift register and a clock frequency of $f_s/4$).

The best identified model in terms of statistical validation was the model identified with X-CLOE using a time-varying forgetting factor with $\lambda_0 = \lambda_1 = 0.95$. The parameters of this model are given in Table 10.3.

It is very important to assess if the model identified in closed loop is better than the model identified in open-loop for describing the behaviour of the closed-loop system using the OLBC controller. Figure 10.9 shows the identified poles of the closed loop (using an RELS algorithm for the closed-loop system identification considered as an input/output map from the excitation to the residual force) and the computed closed-loop poles using the open-loop identified model (OLID-M) and the OLBC controller. Figure 10.10 shows the same type of comparison but the computed closed-loop poles are calculated using the model identified in closed loop (CLID-M). Visual comparison shows clearly that the CLID-M model gives a better description of the real closed-loop system using the OLBC controller (this is obvious in the low frequency range which defines the main behaviour of the closed-loop system in terms of performance).

Table 10.3 Parameters of the model identified in closed-loop

Coeff.	A	Coeff.	B	Coeff.	A	Coeff.	B
a_0	1.0000	b_0	0.0000	a_9	0.6201	b_9	0.2716
a_1	−0.3003	b_1	−0.1556	a_{10}	−0.1095	b_{10}	1.8255
a_2	0.3504	b_2	0.1843	a_{11}	0.1593	b_{11}	1.1575
a_3	−0.6740	b_3	0.5518	a_{12}	−0.1580	b_{12}	1.3638
a_4	−0.2478	b_4	−1.4001	a_{13}	−0.0957	b_{13}	−0.8958
a_5	−0.4929	b_5	3.4935	a_{14}	−0.2030	b_{14}	1.6724
a_6	−0.3217	b_6	−0.3536	a_{15}	–	b_{15}	−1.7691
a_7	0.6157	b_7	−2.7181	a_{16}	–	b_{16}	−0.2240
a_8	0.1459	b_8	−3.0041	–	–	–	–

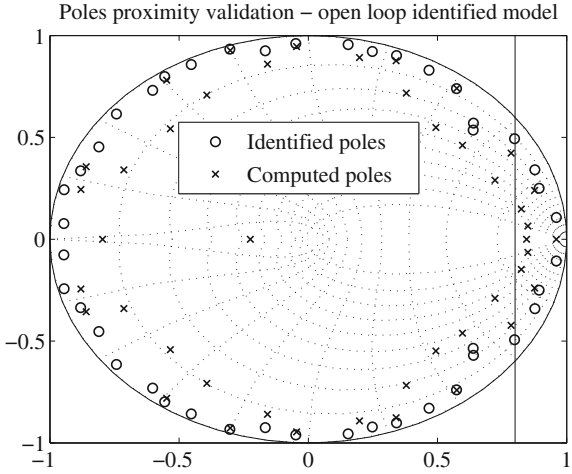

Fig. 10.9 Proximity poles validation of the full order open-loop identified model. Identified and computed closed-loop poles

This is also confirmed by the comparison of the real-time results with the simulated results obtained with the OLID-M model and the CLID-M model (see Fig. 10.11). A small improvement is observed.

10.5 Redesign of the Controller Based on the Model Identified in Closed Loop

Similar to the open-loop situation a reduced order model obtained by balanced truncation will be used. This model has the following dimensions: $n_A = 8$, $n_B = 11$, $d = 0$. The frequency characteristics of this reduced model and those of the full

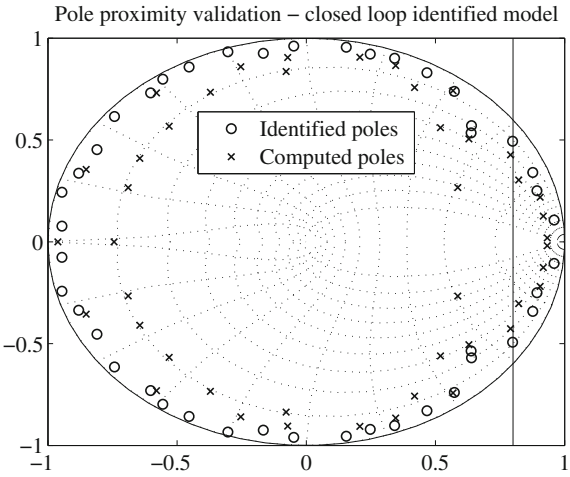

Fig. 10.10 Proximity poles validation of the full order closed-loop identified model. Identified and computed closed-loop poles

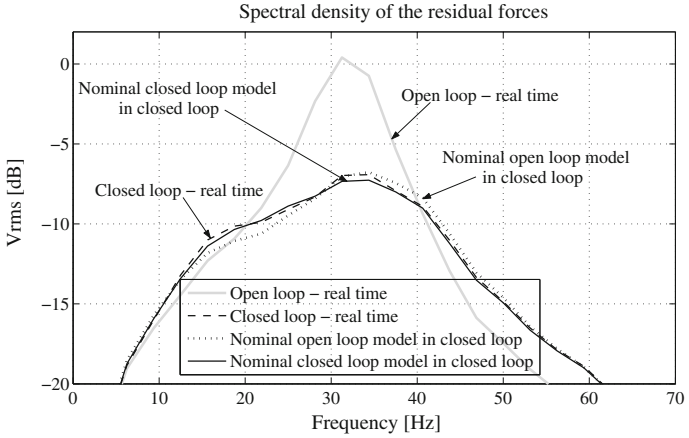

Fig. 10.11 Spectral density of the simulated and real-time closed-loop output (zoom)

order model identified in closed loop are shown in Fig. 10.12.[2] It can be observed that the reduced order model approximates very well the frequency characteristics of the nominal model identified in closed loop in the low frequency range of interest.

Applying the same design procedure based on convex optimization but now using the reduced order model obtained from the nominal model identified in closed loop a new controller (CLBC—Closed-Loop Based Controller) is obtained whose

[2]The option of identifying in closed loop a reduced order model instead of a model of nominal order followed by an order reduction using balanced truncation has provided less good results. For details see [1].

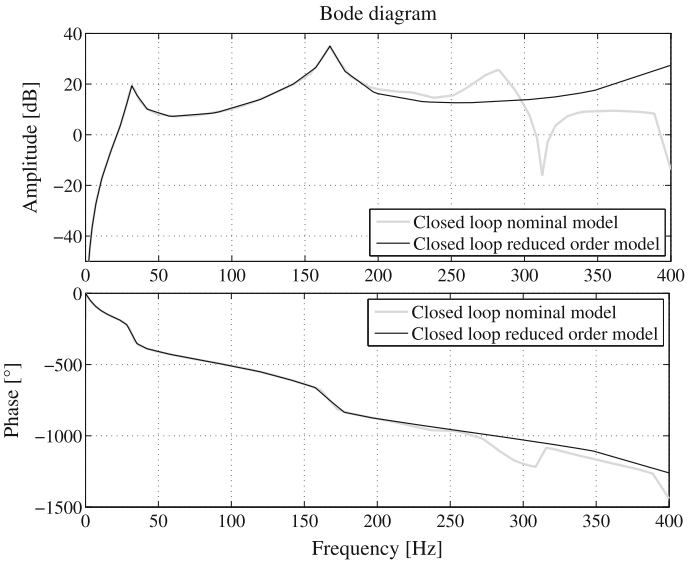

Fig. 10.12 Bode diagram (amplitude and phase) of the nominal model identified in closed-loop operation and of the corresponding reduced order model

parameters are given in Table 10.4. The sensitivity functions with the nominal CLID-M model are shown in Fig. 10.13. The robustness margins are: (1) Modulus Margin $= -3.702$ dB; (2) Delay Margin $= 1.834\, T_S$.

Figure 10.14 shows a comparison of the real-time results obtained with the OLBC controller and with the CLBC (controller based on the closed-loop identified model). The results are very close indicating that already the open-loop identified model was very good.

10.6 Controller Complexity Reduction

Once the CLBC controller is tested and the performance results are satisfactory (see Sect. 10.5), one can pass to the last step of the design methodology presented in Fig. 10.2 which is the reduction of the complexity of the controller.

The techniques for controller complexity reduction by identification in closed loop of the reduced order controller described in Chap. 9 will be used.

One aspect which is very important when reducing the complexity of a controller is that the controller reduction should be done such as to preserve as much as possible the desirable closed-loop properties. Direct simplification of the controller using standard techniques (poles–zeros cancellation within a certain radius, balanced reduction) without taking into account the closed loop behaviour produces in general unsatisfactory results [2, 3].

Table 10.4 Parameters of the controller based on the model identified in closed-loop operation (reduced order model) (CLBC)

Coeff.	R	Coeff.	S	Coeff.	R	Coeff.	S
r_0	0.0195	s_0	1.0000	r_{16}	−0.0488	s_{16}	0.8567
r_1	−0.0618	s_1	−4.5610	r_{17}	0.0446	s_{17}	−0.6306
r_2	0.1030	s_2	9.4917	r_{18}	−0.0495	s_{18}	0.3005
r_3	−0.1238	s_3	−12.4447	r_{19}	0.0437	s_{19}	−0.1080
r_4	0.1263	s_4	12.6103	r_{20}	−0.0255	s_{20}	0.0162
r_5	−0.1087	s_5	−11.5883	r_{21}	0.0078	s_{21}	0.1348
r_6	0.0581	s_6	9.8694	r_{22}	0.0055	s_{22}	−0.2960
r_7	0.0050	s_7	−7.4299	r_{23}	−0.0178	s_{23}	0.3737
r_8	−0.0389	s_8	5.3112	r_{24}	0.0254	s_{24}	−0.3835
r_9	0.0499	s_9	−4.0129	r_{25}	−0.0215	s_{25}	0.3633
r_{10}	−0.0648	s_{10}	2.9544	r_{26}	0.0102	s_{26}	−0.3058
r_{11}	0.0727	s_{11}	−2.1480	r_{27}	−0.0022	s_{27}	0.2004
r_{12}	−0.0602	s_{12}	1.9636	r_{28}	–	s_{28}	−0.0883
r_{13}	0.0511	s_{13}	−1.9125	r_{29}	–	s_{29}	0.0218
r_{14}	−0.0597	s_{14}	1.4914	r_{30}	–	s_{30}	−0.0019
r_{15}	0.0616	s_{15}	−1.0471	–	–	–	–

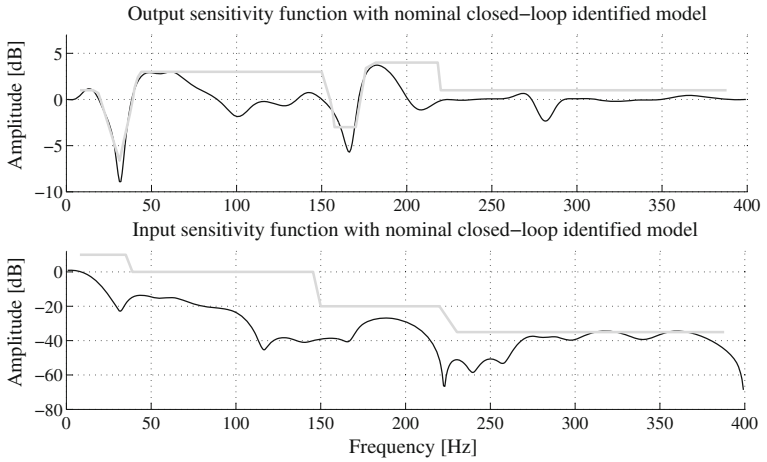

Fig. 10.13 Achieved sensitivity functions (*black thin line*) with the CLBC controller and the nominal model identified in closed-loop operation

The orders of the nominal CLBC controller to be reduced are $n_R = 27$, $n_S = 30$, and its coefficients have been presented in Table 10.4. The model which will be used for the reduction of the controller is the nominal closed-loop identified model

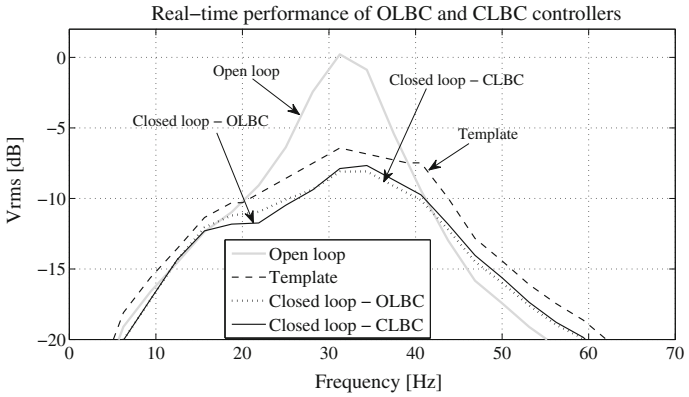

Fig. 10.14 Real-time performance of the OLBC and CLBC controllers (detail)

CLID-M (see Sect. 10.4). The parameters of the model have been given in Table 10.3 (see Sect. 10.4).

Since in active damping we are concerned with attenuation of the disturbances, the main objective for controller reduction will be to obtain an output sensitivity function for the reduced order controller as close as possible to the output sensitivity function obtained with the nominal order controller. As indicated in Chap. 9 and [4], in order to achieve this, the CLOM procedure has to be used. The reduction procedures have been run with simulated data.

A variable forgetting factor with $\lambda_1(0) = 0.95$ and $\lambda_0 = 0.9$ ($\lambda_1(t) = \lambda_0\lambda_1(t - 1) + 1 - \lambda_0$) has been used in the algorithm for the controller parameters estimation. The external input was a PRBS generated by a 9-bit shift register with a $p = 4$ frequency divider (4096 samples). In addition a fixed part $H_R = 1 + q^{-1}$ has been introduced in the reduced order controllers ($R = H_R R'$) which preserves the opening of the loop at 0.5 f_s.

10.6.1 CLOM Algorithm with Simulated Data

Two reduced order controllers have been computed: CLBC-CLOM16 with the orders $n_R = 14$, $n_S = 16$ and CLBC-CLOM5 with the orders $n_R = 4$, $n_S = 5$.

The frequency characteristics of the output and input sensitivity functions (S_{yp} and S_{up}) for the nominal controller CLBC and the two reduced order controllers CLBC-CLOM16 and CLBC-CLOM5 are shown in Figs. 10.15 and 10.16, respectively.

Note that the reduced controller CLBC-CLOM16 corresponds to the complexity of the pole placement controller with the fixed part H_R, while controller CLBC-CLOM5 has a lower complexity.

The values of the various ν-gap are summarized in Table 10.5 (the last two rows give real-time results). It can be remarked that the Vinnicombe stability margins

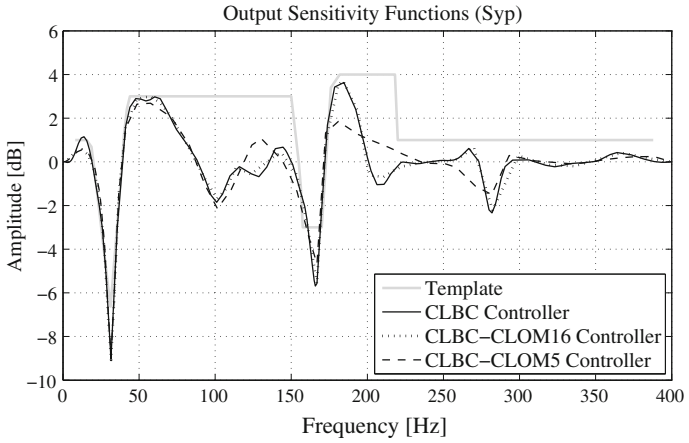

Fig. 10.15 Output sensitivity functions (controller order reduction with CLOM algorithm and simulated data)

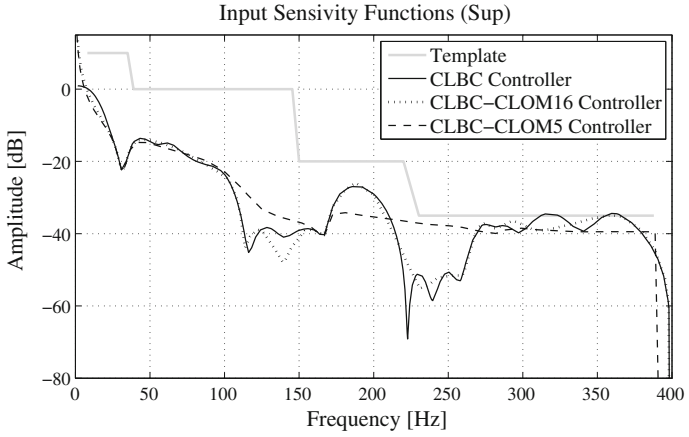

Fig. 10.16 Input sensitivity functions (controller order reduction with CLOM algorithm and simulated data)

$b(K_i, G)$ computed with the nominal model CLID-M for the various reduced order controllers are close to the stability margin obtained with the nominal controller.

The last two rows of Table 10.5 give real-time results. Row 6 gives the ν-gap between the input/output transfer function corresponding to the input sensitivity function S_{up} of the true closed-loop system constituted by the nominal designed controller with the real plant (obtained by system identification between the input r and the output y) and the input/output transfer function of the simulated closed-loop system ($\hat{\hat{S}}_{up}$) constituted by the various controllers (including the nominal one and the reduced ones obtained using simulated data) in feedback connection with the plant

Table 10.5 Comparison of the nominal and reduced order controllers (controller reduction using CLOM algorithm and simulated data)

Controller	*CLBC* $nR = 27$ $nS = 30$	*CLBC-CLOM16* $nR = 14$ $nS = 16$	*CLBC-CLOM5* $nR = 4$ $nS = 5$
$\delta_v(K_n, K_i)$	0	0.6577	0.6511
$\delta_v(S^n_{up}, S^i_{up})$	0	0.6577	0.6511
$\delta_v(S^n_{yp}, S^i_{yp})$	**0**	**0.0386**	**0.1308**
$b(K_i, G)$	0.0303	0.0135	0.0223
$\delta_v(CL(K_n), CL(K_i))$	0.2610	0.2963	0.4275
Closed-loop error variance	0.13582	0.14755	0.17405

model. This quantity is denoted by $\delta_v(CL(K_n), CL(K_i))$. This is a good criterion for the validation of the reduced order controllers in real time. It can be observed that the CLBC-CLOM16 controller gives results which are very close to those of the nominal CLBC controller. Row 7 gives the variance of the residual closed-loop input error between the true system and the simulated one. The results are coherent to those of row 6, showing that CLBC-CLOM16 gives performance very close to those of the nominal controller.

10.6.2 Real-Time Performance Tests for Nominal and Reduced Order Controllers

The spectral densities of the residual forces in open loop and in closed loop corresponding to the nominal controller CLBC and the reduced order ones obtained with the CLOM method (CLBC-CLOM16 and CLBC-CLOM5) are presented in Fig. 10.17.

It can be seen that the performance of reduced order controllers are very close to that of the nominal controller designed using a reduced model of the closed-loop identified model. Note also that the reduction in terms of number of parameters is significant. Very close results have been obtained using the CLIM reduction procedure (see [1, 5]).

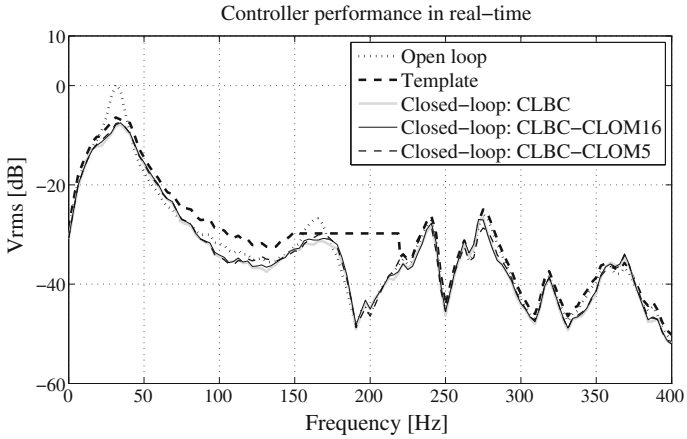

Fig. 10.17 Spectral density of the residual forces in open and closed loop for the nominal and reduced order controllers (CLOM)

10.7 Design of the Controller by Shaping the Sensitivity Function with Band-Stop Filters

The objective of this section is to provide an alternative design procedure for active damping which does not require the use of the convex optimization procedure, but uses only band-stop filters which are iteratively introduced in order to shape the sensitivity functions. This method has been introduced in Sect. 7.2.9. The frequency and damping of the poles of the open-loop identified model are given in Table 6.3.

All asymptotically stable poles will be included as initial desired closed-loop poles. Only the pole located at -0.2177 which corresponds in fact to a pair of damped oscillatory poles near $0.5\,f_s$ will not be included. All the poles remain unchanged in terms of damping, except the complex poles located at 31.939 Hz for which the damping imposed in closed loop will be $\xi = 0.8$ and the complex poles at 164.34 Hz for which a damping of 0.167 will be chosen. These two damped poles will help to satisfy the desired template on the output sensitivity function. 16 real auxiliary poles are assigned at 0.15 (this will not augment the size of the resulting controller).[3]

Figure 10.18 (curve "Controller 1") shows the resulting output sensitivity function S_{yp}. As it can be seen, it almost satisfies the robustness constraints on the modulus margin and delay margin (it is inside the basic template for robustness at all frequencies except around 55 Hz). Nevertheless, when compared to the specification for the output sensitivity function in Fig. 10.19 (dotted line), it can be observed that the desired disturbance attenuation is not satisfied. The input sensitivity function satisfies the specified template, see Fig. 10.20.

[3]The design using BSF has been done with iReg software which provides a convenient interactive environment.

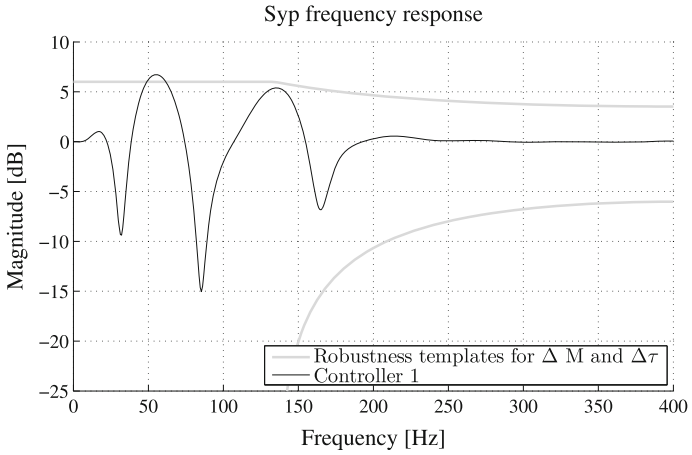

Fig. 10.18 Output sensitivity function for the Controller 1 (with modulus and delay margin templates)

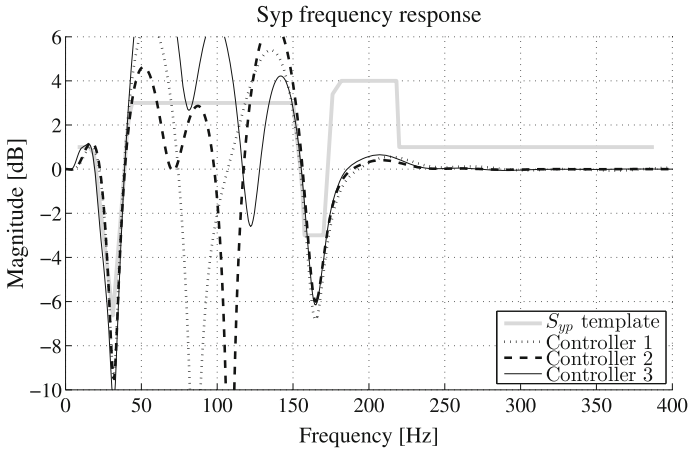

Fig. 10.19 Output sensitivity function with the three initial controllers

To have zero gain on the input sensitivity function at $0.5 f_s$, one zero at -1 is added to the fixed part of the controller numerator by including into H_R the first order polynomial $(1+q^{-1})$. One more characteristic pole at 0.15 is then added (this will not increase the order of the controller but avoid to have a pole assigned to 0). The result can be seen in Figs. 10.19 and 10.20, "Controller 2" curve. One can see that the template is still violated in several frequency regions.

For shaping the output sensitivity function in the frequency region of the first attenuation mode around 30 Hz three BSF have been added at 14, 24 and 38.7 Hz, with attenuation of -2.5, -7 and -5.5 dB respectively. The resulting controller sensitivity functions are shown in Figs. 10.19 and 10.20 (curve "Controller 3"). The

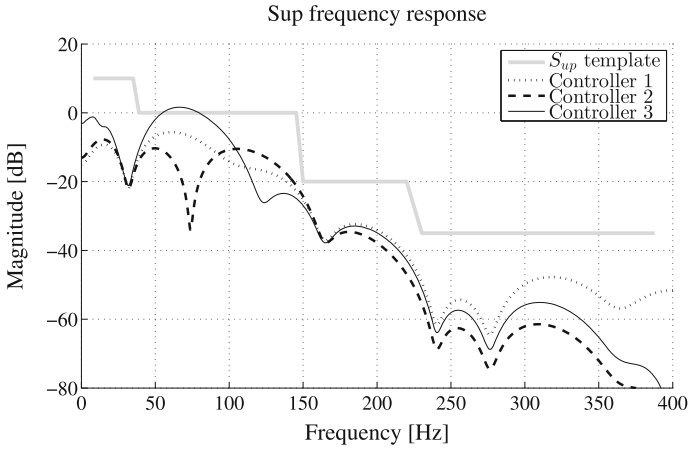

Fig. 10.20 Input sensitivity function with the three initial controllers

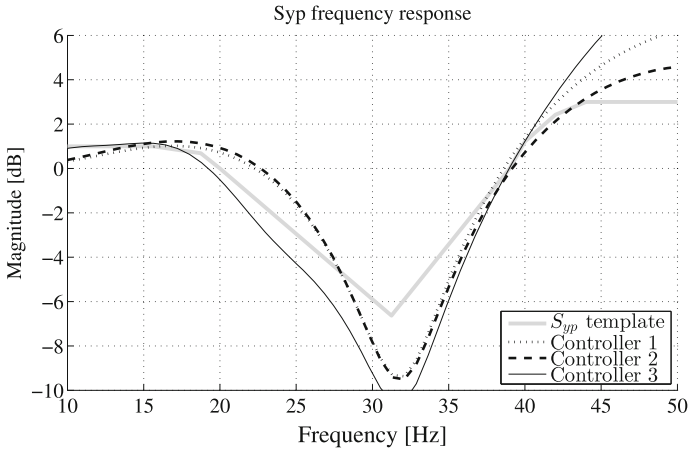

Fig. 10.21 Output sensitivity function with the three initial controllers (zoom)

result in the region of the first attenuation mode around 30 Hz can be better evaluated using Fig. 10.21, where a zoom between 10 and 50 Hz is shown. For all three BSF, the denominator damping has been chosen equal to 0.5. It can be observed that "Controller 3" satisfies the imposed template in the lower frequency region below 30 Hz.

The final design step is to improve the shape of the sensitivity functions at the other frequencies. Two additional BSF have been added for shaping the output sensitivity function and five for shaping the input sensitivity function. In addition, the initial three BSF have been slightly modified as each newly added BSF has, however, a slight influence at neighbouring frequencies. Tables 10.6 and 10.7 summarize the characteristics of the various BSF. A sensitivity functions comparison between

Table 10.6 Band-stop filters for the output sensitivity function

Controller number	Frequency (Hz)	Attenuation (dB)	Denominator damping
1	14	−9.1	0.95
2	23.5	−14.759	0.95
3	41.158	−5.2	0.5
4	69.45	−15.11	0.95
5	132.5	−14.759	0.95

Table 10.7 Band-stop filters for the input sensitivity function

Controller number	Frequency (Hz)	Attenuation (dB)	Denominator damping
1	51.5	−16	0.95
2	70.74	−14.052	0.5
3	92.6	−15.1	0.95
4	115.76	−9.1	0.5
5	313.826	−2.733	0.95

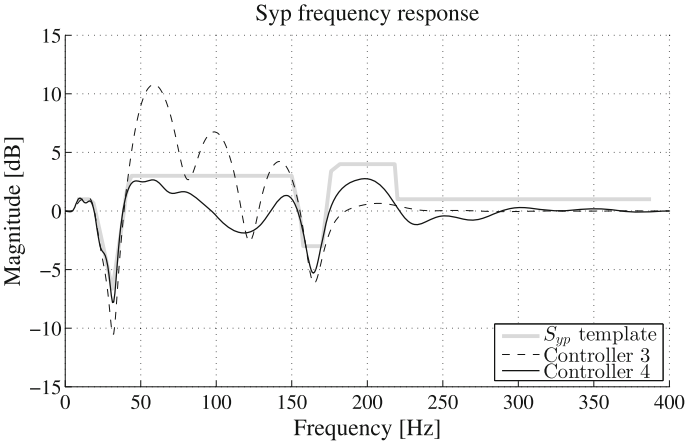

Fig. 10.22 Output sensitivity function comparison between "Controller 3" and "Controller 4"

"Controller 3" and "Controller 4" is given in Figs. 10.22 (output sensitivity functions) and 10.23 (input sensitivity functions).

Finally, Figs. 10.24 and 10.25 give a comparison of "Controller 4" and the controller designed using convex optimization (see previous sections). A zoom between 10 and 50 Hz is shown in Fig. 10.26 for comparative evaluation of the obtained characteristics around the first attenuation region. As it can be seen, both controllers satisfy the template in the low frequency region while in the high frequency region

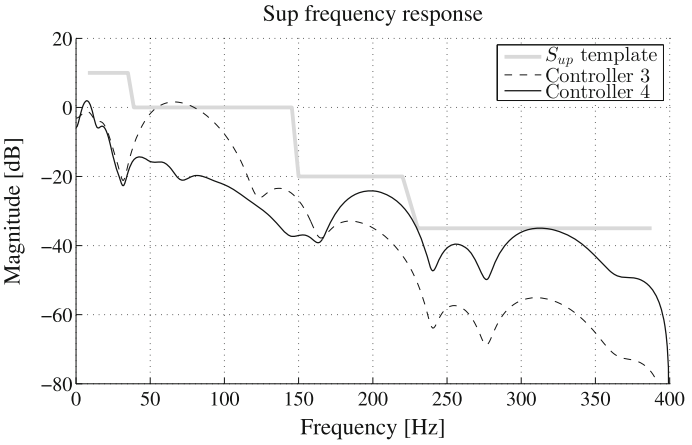

Fig. 10.23 Input sensitivity function comparison between "Controller 3" and "Controller 4"

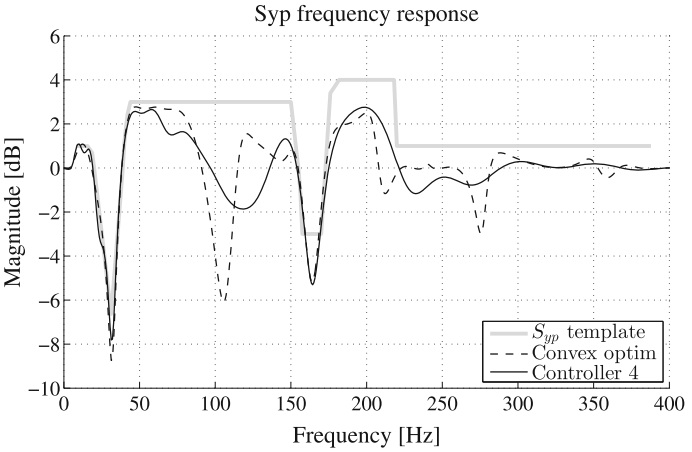

Fig. 10.24 Output sensitivity function comparison between the convex optimization controller and "Controller 4" obtained using iREG

the controller designed by convex optimization slightly exceeds the imposed template. Concerning their complexity, "Controller 4" designed using BSF filters has 71 parameters ($n_R = 34$ and $n_S = 36$) while the controller designed by convex optimization has 58 parameters ($n_R = 27$ and $n_S = 30$).

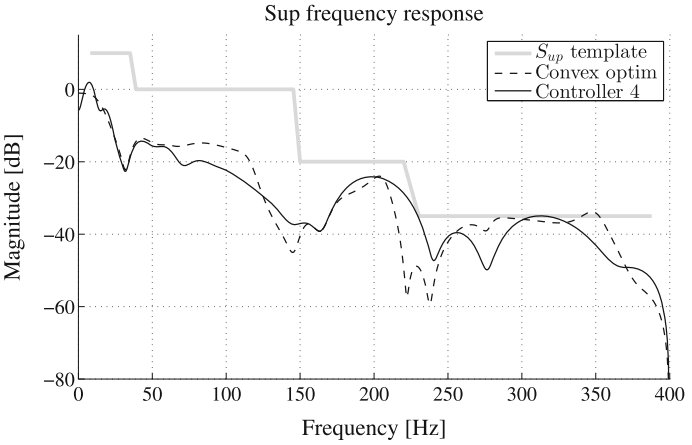

Fig. 10.25 Input sensitivity function comparison between the convex optimization controller and "Controller 4" obtained using iREG

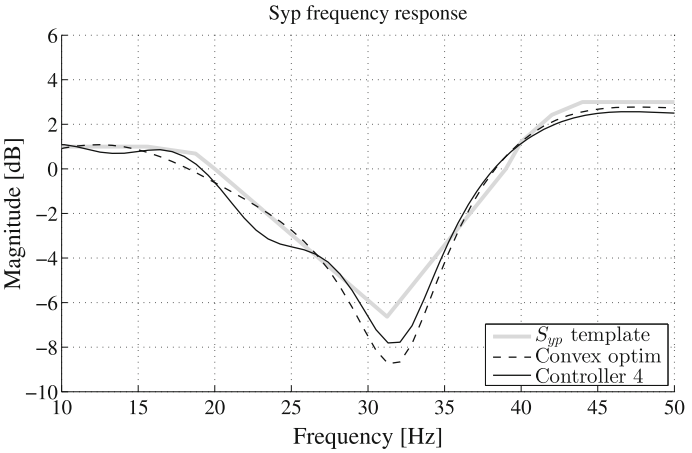

Fig. 10.26 Output sensitivity function comparison between the convex optimization controller and "Controller 4" obtained using iREG (zoom)

10.8 Concluding Remarks

- The design of active damping systems consists of the following major steps:
  - Definition of the control performance specifications in the frequency domain.
  - Design of the controller ensuring the desired performance.
  - Validation of the controller.
- Design of the controller for active damping include several steps:

  - Open-loop identification of the secondary path.
  - Design of the controller based on the secondary path model identified in open-loop operation.
  - Implementation and validation of the controller.
- If the performance is not satisfactory, the following procedure has to be followed:
  - Identification in closed-loop operation of a new model for the secondary path and validation of the identified model.
  - Redesign of the controller on the basis of the model identified in closed loop.
  - Implementation and validation of the controller designed on the basis of the model identified in closed-loop operation.
- The effective design of the controller requires the shaping of the sensitivity functions.
- Shaping of the sensitivity functions can be achieved using convex optimization or band-stop filters combined with poles placement.
- If constraints on the computational load exist, the final step in the design is the reduction of the controller complexity with the objective of preserving the closed-loop performance.
- The reduced order controller should be implemented and validated.

10.9 Notes and References

Active damping for disturbance attenuation and control of lightly damped structures which has different objectives use, however, similar feedback techniques [6].

Suspension bridges and cable-stayed bridges require active damping to reduce the effects of various phenomena. Active damping solutions have been proposed in [7–14]. Active tendon control of cable-stayed bridges using hydraulic suspension is considered in [11].

An important issue in active damping is the construction of physical systems allowing to achieve active damping. Use of piezoelectric devices is a very efficient approach for many applications. See [14] for a survey and [8] for a detailed modelling of this type of devices. Applications of piezoelectric devices for active damping have been reported for: (i) Large space structures [14], (ii) Wafer stepper in lithography [15] and (iii) Active tendon control of cable structures in space [16, 17].

Other references related to active damping include [18–21].

A key issue in active damping is a careful shaping of the sensitivity functions. Other techniques than those presented in this chapter can be used. H_∞ where the shaping of the sensitivity function is converted in a weighted frequency criterion minimization can be considered [22, 23]. Linear-Quadratic Control with frequency weighting can also be considered [24].

References

1. Constantinescu A (2001) Commande robuste et adaptative d'une suspension active. Thèse de doctorat, Institut National Polytechnique de Grenoble
2. Anderson B, Liu Y (1989) Controller reduction: concepts and approaches. IEEE Trans Autom Control 34(8):802–812
3. Anderson B (1993) Controller design: moving from theory to practice. IEEE Control Mag 13:16–25
4. Landau I, Karimi A (2002) A unified approach to model estimation and controller reduction (duality and coherence). Eur J Control 8(6):561–572
5. Landau I, Karimi A, Constantinescu A (2001) Direct controller order reduction by identification in closed loop. Automatica 37:1689–1702
6. Karkosch HJ, Preumont A (2002) Recent advances in active damping and vibration control. Actuator 2002, 8th International Conference on New ActuatorsBremen, Germany, pp 248–253
7. Cannon RJ, Rosenthal D (1984) Experiments in control of flexible structures with noncolocated sensors and actuators. J Guid Control Dyn 7(5):546–553
8. Preumont A (2011) Vibration control of active structures - an introduction. Springer, Berlin
9. Achkire Y, Preumont A (1996) Active tendon control of cable-stayed bridges. Earthq Eng Struct Dyn 25(6):585–597
10. Achkire Y, Bossens F, Preumont A (1998) Active damping and flutter control of cable-stayed bridges. J Wind Eng Ind Aerodyn 74–76:913–921
11. Bossens F, Preumont A (2001) Active tendon control of cable-stayed bridges: a large-scale demonstration. Earthq Eng Struct Dyn 30(7):961–979
12. Auperin M, Dumoulin C (2001) Structural control: point of view of a civil engineering company in the field of cable-supported structures. In: Casciati F, Magonette G (eds) Structural control for civil and infrastructure engineering. Singapore, pp 49–58
13. Preumont A, Dufour JP, Malekian C (2015) An investigation of the active damping of suspension bridges. Math Mech Complex Syst 3(4):385–406
14. Preumont A, Dufour JP, Malekian C (1992) Active damping by a local force feedback with piezoelectric actuators. J Guid Control Dyn 15(2):390–395
15. Jansen B (2000) Smart disk tuning and application in an ASML wafer stepper. Msc. thesis, Control Laboratory, University of Twente, Enschede, The Netherlands
16. Preumont A, Achkire Y, Bossens F (2000) Active tendon control of large trusses. AIAA J 38(3):493–498
17. Preumont A, Bossens F (2000) Active tendon control of vibration of truss structures: theory and experiments. J Intell Mat Syst Struct 2(11):91–99
18. Preumont A, Loix N (1994) Active damping of a stiff beam-like structure with acceleration feedback. Exp Mech. 34(1):23–26
19. Preumont A, Achkire Y (1997) Active damping of structures with guy cables. J Guid Control Dyn 20(2):320–326
20. Chen X, Jiang T, Tomizuka M (2015) Pseudo Youla-Kučera parameterization with control of the waterbed effect for local loop shaping. Automatica 62:177–183
21. Sievers LA, von Flotow AH (1988) Linear control design for active vibration isolation of narrow band disturbances. In: Proceedings of the 27th IEEE Conference on Decision and Control 1988. IEEE, pp 1032–1037
22. Zhou K, Doyle J (1998) Essentials of robust control. Prentice-Hall International, Upper Saddle River
23. Alma M, Martinez J, Landau I, Buche G (2012) Design and tuning of reduced order H_∞ feedforward compensators for active vibration control. IEEE Trans Control Syst Technol 20(2):554–561. doi:10.1109/TCST.2011.2119485
24. Tharp H, Medanic J, Perkins W (1988) Parameterization of frequency weighting for a two-stage linear quadratic regulator based design. Automatica 24(5):415–418